Thermodynamics of Aminoglycoside Binding to Aminoglycoside-3′-phosphotransferase IIIa Studied by Isothermal Titration Calorimetry†

Can Özen‡ and Engin H. Serpersu*,‡,§

Graduate School of Genome Science and Technology, Department of Biochemistry and Cellular and Molecular Biology, and Center of Excellence in Structural Biology, University of Tennessee, Knoxville, Tennessee 37996

Received June 18, 2004; Revised Manuscript Received September 3, 2004

ABSTRACT: The aminoglycoside-3′-phosphotransferase IIIa [APH(3′)-IIIa] phosphorylates aminoglycoside antibiotics and renders them ineffective against bacteria. APH(3′)-IIIa is the most promiscuous aminoglycoside phosphotransferase enzyme, and it modifies more than 10 different aminoglycoside antibiotics. A wealth of information exists about the enzyme; however, thermodynamic properties of enzyme−aminoglycoside complexes are still not known. This study describes the determination of the thermodynamic parameters of the binary enzyme−aminoglycoside and the ternary enzyme−metal-ATP−aminoglycoside complexes of structurally related aminoglycosides using isothermal titration calorimetry. Formation of the binary enzyme−aminoglycoside complexes is enthalpically driven and exhibits a strongly disfavored entropic contribution. Formation of the ternary enzyme−metal-ATP−aminoglycoside complexes yields much smaller negative ΔH values and more favorable entropic contributions. The presence of metal-ATP generally increases the affinity of aminoglycosides to the enzyme. This is consistent with the kinetic mechanism of the enzyme in which ordered binding of substrates occurs. However, the observed ΔH values neither correlate with kinetic parameters k_{cat}, K_m, and k_{cat}/K_m nor correlate with the molecular size of the substrates. Comparison of the thermodynamic properties of the complexes formed by structurally similar aminoglycosides indicated that the 2′- and the 6′-amino groups of the substrates are involved in binding to the enzyme. Thermodynamic properties of the complexes formed by aminoglycosides differing only at the 3′-hydroxyl group suggested that the absence of this group does not alter the thermodynamic parameters of the ternary APH(3′)-IIIa−metal-ATP−aminoglycoside complex. Our results also indicate that protonation of ligand and protein ionizable groups is coupled to the complex formation between aminoglycosides and APH(3′)-IIIa. Comparison of ΔH values for different aminoglycoside−enzyme complexes indicates that enzyme and substrates undergo significant conformational changes in complex formation.

Aminoglycoside antibiotics are highly potent, wide-spectrum bactericidals (*1*−*3*). Since the discovery of streptomycin in 1943, they have been successfully used in treatment of various important bacterial infections such as tuberculosis and the plague. Aminoglycosides target the 16S rRNA of the 30S ribosomal subunit and interfere with its translational fidelity and the translocation step of protein synthesis, eventually resulting in cell death (*1*, *4*). Aminoglycosides are hydrophilic molecules carrying several hydroxyl and amino functional groups. Most of the aminoglycosides have one or more amino sugars that are attached to a 2-deoxystreptamine (2-DOS)[1] ring. Aminoglycosides that contain 2-DOS are generally further separated into two groups, the neomycin group (4,5-disubstituted 2-DOS) and the kanamycin group (4,6-disubstituted 2-DOS), based on the substitution pattern of the 2-DOS (Figure 1).

As for any antibiotic drug in use, bacterial resistance is the major problem in clinical effectiveness of aminoglycosides. Covalent modification is the most frequent mode of resistance among several resistance mechanisms employed by resistant pathogens (*3*, *5*). Three families of aminoglycoside-modifying enzymes, containing more than 50 members, have been identified so far. On the basis of the modification reaction catalyzed, enzymes are designated as *O*-phosphotransferases, *N*-acetyltransferases, and *N*-nucleotidyltransferases. Some of these enzymes are highly promiscuous in substrate selection and have different regioselectivity for covalent modification (*3*, *5*, *6*).

Aminoglycoside phosphotransferases carry out ATP-dependent phosphorylation of cognate aminoglycoside hy-

† This research was supported by a grant from the National Science Foundation (MCB 01110741 to E.H.S.).

* Correspondence should be sent to to this author at the Department of Biochemistry and Cellular and Molecular Biology, University of Tennessee, Walters Life Sciences Building M407, Knoxville, TN 37996-0840. Tel: 865-974-2668. Fax: 865-974-6306. E-mail: Serpersu@utk.edu.

‡ Graduate School of Genome Science and Technology, University of Tennessee.

§ Department of Biochemistry and Cellular and Molecular Biology and Center of Excellence in Structural Biology, University of Tennessee.

[1] Abbreviations: 2-DOS, 2-deoxystreptamine; APH(3′)-IIIa, aminoglycoside-3′-phosphotransferase IIIa; ITC, isothermal titration calorimetry.

10.1021/bi0487286 CCC: $27.50
Published on Web 10/27/2004

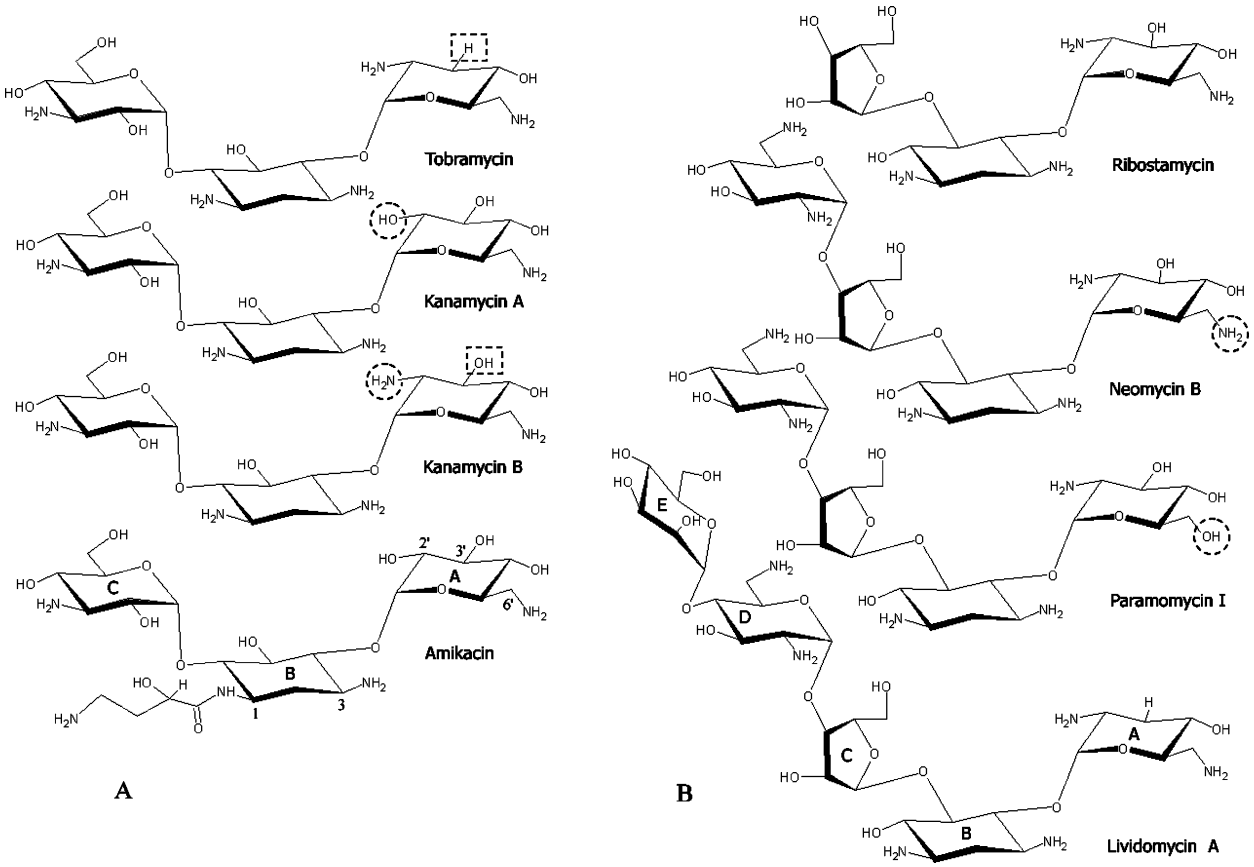

FIGURE 1: Structures of aminoglycosides containing a (A) 4,6-disubstituted or (B) 4,5-disubsituted 2-DOS ring. Single functional group differences between structurally similar aminoglycosides are indicated with dotted circles marking the 2′- and 6′-positions in (A) and (B), respectively. Dotted squares in (A) show the 3′-position. Rings A, B, C, D, and E are also named as primed (′), unprimed, double primed (″), triple primed (‴), and quadruple primed (⁗) respectively. The numbering of carbon atom positions is shown on the amikacin structure.

droxyl groups. The aminoglycoside-3′-phosphotransferase IIIa [APH(3′)-IIIa] has the broadest substrate specificity within the 3′-subfamily of the aminoglycoside-modifying enzymes (*7*). The enzyme has been extensively studied mainly by kinetic and crystallographic methods (*8*−*12*), and the crystal structures of enzyme−MgADP−aminoglycoside complexes are available with kanamycin A and neomycin B (*7*). Enzyme-bound conformations of several aminoglycosides were also determined by NMR spectroscopy in our laboratory (*13*−*17*). Although APH(3′)-IIIa is an extensively studied and relatively well-characterized aminoglycoside kinase, thermodynamic properties of its complexes with aminoglycosides have not previously been described. To the best of our knowledge, there is only one study describing binding of nucleotide ligands to APH(3′)-IIIa (*18*). In this paper, we report the thermodynamic characterization of binary APH(3′)-IIIa−aminoglycoside and ternary APH(3′)-IIIa−metal-ATP−aminoglycoside complexes studied by isothermal titration calorimetry (ITC) using aminoglycosides containing a 4,5- or a 4,6-disubstituted 2-DOS ring. Preliminary results of this work were presented earlier (*19*).

MATERIALS AND METHODS

Aminoglycoside antibiotics, adenosine 5′-triphosphate (ATP), and all other chemicals were of highest available purity and were obtained from Sigma (St. Louis, MO). The strong anion-exchange medium POROS 20HQ was purchased from Applied Biosystems (Foster City, CA).

Protein Purification. APH(3′)-IIIa was expressed in *Escherichia coli* BL21(DE3) carrying the overexpression plasmid pETPCR6, which was provided by Dr. Gerard D. Wright. APH(3′)-IIIa was purified using a modified version of the original procedure described by McKay et al. (*8*). Ten liters of Luria broth (LB) media in a New Brunswick (Edison, NJ) BioFlo 110 fermentor vessel was inoculated with a 100 mL overnight grown subculture. The cells were grown at 37 °C. The culture was induced at the mid log phase (OD_{600} = 0.6) with 1 mM final concentration of IPTG. After a 5 h induction period, the culture was divided into 1.5 L fractions, and then the cells were harvested by centrifugation. Each fraction was solubilized in 35 mL of lysis buffer (50 mM Tris, 5 mM EDTA, 200 mM NaCl, 1 mM PMSF, 0.2 mM DTT) and lysed by three to four passages through a French press at 16000 psi. Cell debris was removed by centrifugation, and the supernatant was diluted to 50 mL with buffer A (50 mM Tris, 1 mM EDTA, pH 8.0) before loading it onto a strong anion-exchange POROS 20HQ column (250 × 4.6 mm) attached to a BIOCAD 700E perfusion chromatography workstation from Applied Biosystems. After the cell hydrolysate was loaded, the column was washed with four column volumes of buffer A. A linear gradient of 0−20% buffer B in buffer A was applied through five column volumes to elute contaminant proteins. The pure APH(3′)-IIIa was then eluted with two column volumes of 20% buffer B in buffer A. Pooled fractions were dialyzed against buffer A, freeze-dried, and stored at −80 °C. The purity of the enzyme was >98% as judged by SDS−PAGE.

The activity of the enzyme was determined by using a coupled-enzyme assay as described previously (*8*).

ITC Experiments. Isothermal titration calorimetry experiments were performed at 37 °C using a VP-ITC microcalorimeter from Microcal, Inc. (Northampton, MA). Measurements were carried out in 50 mM Tris or Bicine buffers which also contained 100 mM KCl at pH values of 7.5 and 8.5. Enzyme preparations were dialyzed extensively against buffer, and ligand solutions were prepared in the final dialyzate. Both solutions were degassed under vacuum for 10 min. Titrations consisted of 29 injections programmed as 10 μL per injection and separated by 240 s. Cell stirring speed was 300 rpm.

Binary complex titrations were performed by titrating 0.75−3.0 mM aminoglycoside solution into a solution containing 50−100 μM APH(3′)-IIIa in the sample cell. To obtain reliable dissociation constants, the *c*-value, a parameter obtained by the multiplication of the association constant and the total concentration of ligand binding sites (*20*), was kept between 10 and 100 for all titrations. Due to tight binding of neomycin B and paromomycin I (*c*-values were ∼600 at 80 μM enzyme concentration), the ternary titrations with these antibiotics were repeated at 10 μM enzyme concentration for more accurate determination of the dissociation constants. $CaCl_2$ (1.5 mM) and ATP (1.0 mM) were present in the syringe and sample cell during ternary complex titrations. Control runs were performed by titrating ligands to buffer, and the resulting reference signal was subtracted from corresponding experimental data. The enzymatic activity of APH(3′)-IIIa was tested before and after titrations, and no loss of activity was detected.

Thermodynamic parameters N (stoichiometry), K_A (association constant), and ΔH (enthalpy change) were obtained by nonlinear least-squares fitting of experimental data using a single-site binding model of the Origin software package (version 5.0) provided with the instrument. The free energy of binding (ΔG) and entropy change (ΔS) were obtained using the equations:

$$\Delta G = -RT \ln K_A \quad (1)$$

$$\Delta G = \Delta H - T\Delta S \quad (2)$$

The affinity of the aminoglycoside to the enzyme and enzyme−CaATP complex is given as the dissociation constant ($K_D = 1/K_A$). CaATP, a competitive inhibitor of the enzyme (*13*), was used instead of MgATP to prevent product formation in the ternary titrations.

RESULTS AND DISCUSSION

ITC is a direct method for characterizing the stoichiometry, affinity, and enthalpy of binding reactions in solution (*21*−*23*) and has been employed in binding studies of saccharides with their partner lectins (*24*−*26*) or proteins (*27*), or aminoglycoside−RNA complexes (*28*), aminoglycoside−acetyltransferase interactions (*29*), and nucleotide binding to APH(3′)-IIIa (*18*). In this study, we used ITC to determine the thermodynamic parameters for aminoglycoside binding to APH(3′)-IIIa in the presence and absence of CaATP. Several aminoglycosides with 4,5- and 4,6-disubstituted 2-deoxystreptamine rings were used in binding studies (Figure 1).

Table 1: Thermodynamic Parameters for Aminoglycoside Binding to APH(3′)-IIIa (Binary Complex) at pH 7.5[a]

	buffer	K_D (μM)	ΔH_{obs} (kcal/mol)	ΔH_{int}[b] (kcal/mol)	$-T\Delta S$ (kcal/mol)	ΔG (kcal/mol)
kanamycin A	Tris	6.2	−33.0	−44.9	25.6	−7.4
	Bicine	4.6	−38.3		30.8	−7.5
kanamycin B	Tris	0.3	−22.4	−41.3	13.2	−9.2
	Bicine	0.5	−30.8		21.8	−9.0
tobramycin	Tris	0.8	−29.2	−47.0	20.5	−8.7
	Bicine	0.6	−37.1		28.3	−8.8
amikacin	Tris	92.6	−19.5	−17.9	13.8	−5.7
	Bicine	43.5	−18.8		12.6	−6.2
ribostamycin	Tris	1.7	−30.1	−25.6	22.0	−8.1
	Bicine	1.9	−28.1		20.0	−8.1
neomycin B	Tris	0.26	−33.4	−55.7	24.1	−9.3
	Bicine	0.30	−43.3		34.0	−9.3
paromomycin I	Tris	0.44	−30.4	−43.9	21.4	−9.0
	Bicine	0.30	−36.4		27.1	−9.3
lividomycin A	Tris	0.81	−33.6	−57.3	25.0	−8.6
	Bicine	0.57	−44.1		35.3	−8.8

[a] Determined at 310 K. K_D values were calculated from ITC-derived K_A. Fitting errors: K_D, 2−12%; ΔH, 0.2−3%. The stoichiometry of complex formation was 1.0 ± 0.2 in all titrations. [b] Intrinsic enthalpy changes (ΔH_{int}) were calculated using eqs 3a and 3b.

In general, the binding of aminoglycosides to APH(3′)-IIIa is an enthalpically driven process accompanied by an unfavorable entropic contribution. Negative ΔH values associated with the formation of binary APH(3′)-IIIa−aminoglycoside and ternary APH(3′)-IIIa−CaATP−aminoglycoside complexes suggest that favorable binding contacts such as polar, electrostatic, van der Waals, and hydrogen bonds exist between aminoglycosides and APH(3′)-IIIa. Exothermic heat and binding affinities were not, however, proportional with the size of aminoglycosides (i.e., larger aminoglycosides did not necessarily exhibit greater heats of association or tighter binding). Also, there was no correlation between the heat of binding and the kinetic parameters K_m, k_{cat}, or k_{cat}/K_m.

Binary Enzyme−Aminoglycoside Complexes. Results summarized in Table 1 show that formation of APH(3′)-IIIa−aminoglycoside complexes exhibits large, exothermic heats of association, and they are entropically disfavored. This observation indicates that the sum of total binding entropy due to solvation effects and to the rotational, translational, and configurational freedoms of aminoglycosides and APH(3′)-IIIa was greatly reduced as a result of complex formation. However, the large exothermic heats of association compensate the entropic penalty to yield negative ΔG values in each case. In all cases, the best fits were obtained with a single-site model. Figure 2 shows the titration isotherms obtained for binary titrations of APH(3′)-IIIa with the tightest (neomycin B) and the weakest (amikacin) binding aminoglycosides. The differences between the heats of association and the binding affinities of the two aminoglycosides are clearly visible in this figure.

There were no clear trends with respect to dissociation constant (K_D) or other thermodynamic parameters to distinguish aminoglycosides with the 4,5- or 4,6-disubstituted 2-DOS rings from each other. While K_D values varied ∼400-fold, ΔH_{obs} values were between −18.8 and −44.1 kcal/mol, and $T\Delta S$ values were between −12.6 and −35.3 kcal/mol. Overall, however, all binary enzyme−aminoglycoside complexes gave negative ΔG values. Also, with the exception

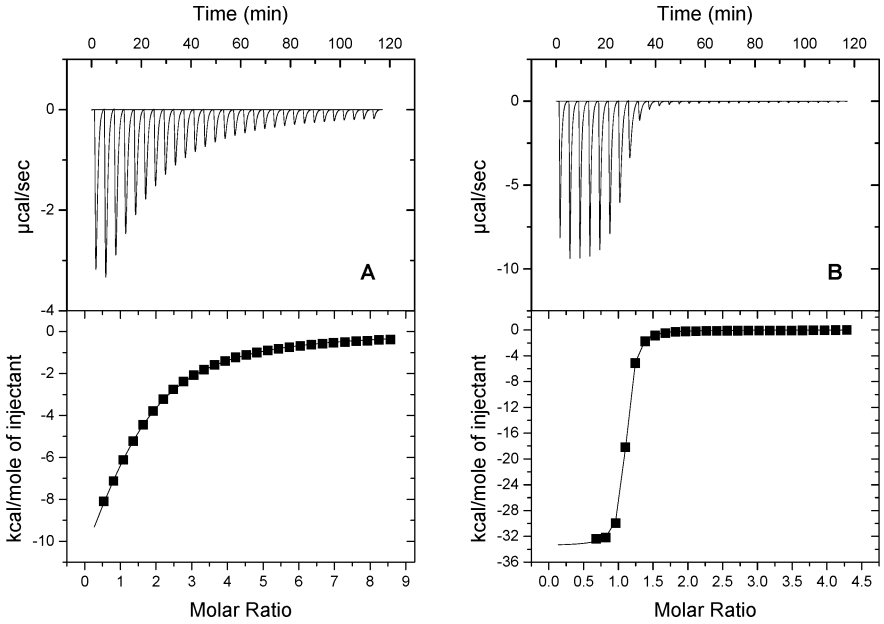

FIGURE 2: Isotherms of (A) 3.0 mM amikacin and (B) 1.5 mM neomycin B titration to 80 μM APH(3′)-IIIa. All solutions contained 50 mM Tris, pH 7.5, and 100 mM KCl, and titrations were performed at 310 K. The upper panel shows the raw data (thermal power). Time integration of the thermal power yields the heat of injection, which is plotted against the molar ratio of ligand to enzyme in the lower panel. The solid line in bottom panel represents the least-squares fitting of the data to a one-site binding model.

of amikacin, all ΔG values were within 1.8 kcal/mol. The results observed with amikacin are somewhat expected since amikacin is one of the worst substrates of APH(3′)-IIIa (high K_m, low k_{cat}, and k_{cat}/K_m) with the lowest affinity and the smallest negative ΔG among the aminoglycosides tested. Amikacin has a bulky group attached to the N-1 of the 2-DOS ring (Figure 1), which may interfere with the interaction of aminoglycoside with the enzyme. This may explain why amikacin is still a clinically useful antibiotic.

Observed ΔH values were different for the same complex when titrations were performed in buffers with different heats of ionization [Tris, 11.7 kcal/mol (*30*), vs Bicine, 6.5 kcal/mol (*31*)]. This observation indicates that the formation of enzyme−aminoglycoside complexes causes shifts in pK_a of ionizable groups and further protonation/deprotonation occurs in the complex. The data obtained in two different buffers then can be used to determine the intrinsic enthalpy changes (ΔH_{int}) and net number of binding-coupled protons (Δn) for aminoglycoside−APH binary complex formation. These values were calculated by simultaneous solution of the equations (*32*):

$$\Delta H_{obs1} = \Delta H_{int} + \Delta H_{ion1}\Delta n \quad (3a)$$

$$\Delta H_{obs2} = \Delta H_{int} + \Delta H_{ion2}\Delta n \quad (3b)$$

where ΔH_{obs} is the observed enthalpy change, ΔH_{ion} is the ionization enthalpy change for the particular buffer used, and Δn is the net number of protons released or absorbed by the buffer upon complex formation. Positive values of the determined Δn for the formation of the binary enzyme−aminoglycoside complexes with kanamycin A, kanamycin B, tobramycin, neomycin B, paramomycin, and lividomycin A indicate binding-coupled protonation whereas negative values observed for ribostamycin and amikacin are due to the deprotonation of ligand and/or protein groups.

The data shown in Table 1 also indicate that ΔH_{int} values show a large variation for different aminoglycosides (more than ~3-fold). In addition, as shown in Table 2, the observed Δn values for the binary enzyme−aminoglycoside complexes with neomycin B and lividomycin A exceed the total fraction of $-NH_2$ groups on these ligands. Thus, additional protonation must occur in the enzyme side chains. Also, the comparison of Δn values of kanamycin A and kanamycin B shows that the difference ($\Delta\Delta n$) is 0.6. The only difference between these two antibiotics is the presence of an amino (kanamycin B) vs hydroxyl (kanamycin A) at the 2′-position. However, the protonation of this group alone cannot be responsible for the observed Δn with kanamycin B, because it is already 92% protonated at pH 7.5. Similarly, the comparison of the complexes of neomycin B and ribostamycin shows a $\Delta\Delta n$ value of 2.28, which exceeds the differences in the fraction of $-NH_2$ groups of two antibiotics. These observations suggest that not only does the ionization of enzyme side chains contribute to the observed heat of the complex formation but the contribution is different for every aminoglycoside. These are in excellent agreement with the results obtained by NMR studies. Heteronuclear $^1H-^{15}N$ HSQC spectra acquired with enzyme−aminoglycoside complexes using ^{15}N-enriched enzyme showed that different sets

Table 2: Protonation Coupled to Aminoglycoside Binding to APH(3′)-IIIa (Binary Complex) at pH 7.5

	total fraction of NH_2[a]	Δn[b]
kanamycin A	2.51	1.02
kanamycin B	2.59	1.62
tobramycin	2.59	1.52
amikacin	1.25	−0.13
ribostamycin	1.71	−0.38
neomycin B	1.15	1.90
paromomycin I	1.18	1.15
lividomycin A	1.14	2.03

[a] The total fraction of deprotonated amino groups was calculated on the basis of the determined pK_a values of aminoglycosides (*14*, *28*, *33*). [b] The net number of binding-coupled protons was calculated using eqs 3a and 3b.

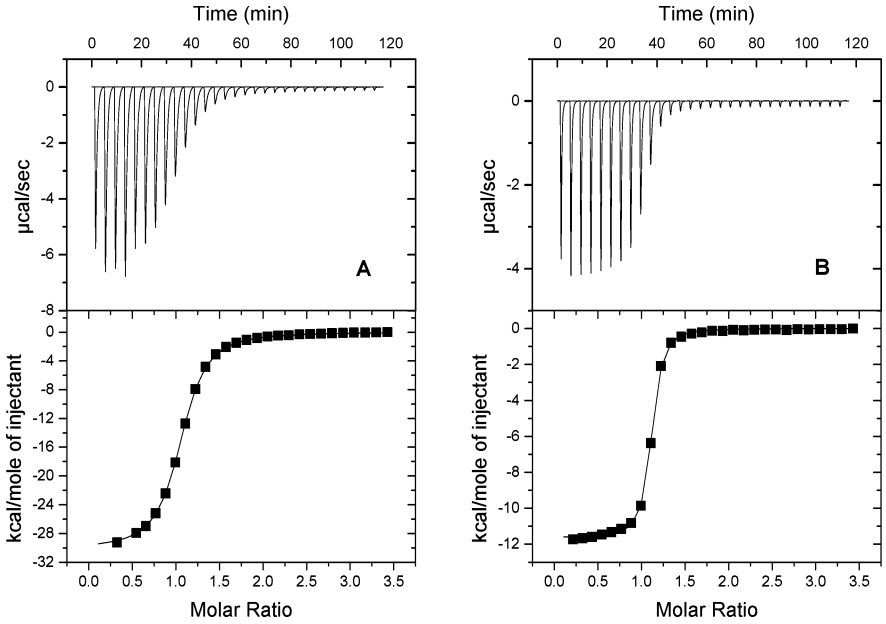

FIGURE 3: ITC profiles of 1.2 mM ribostamycin titration to 80 μM APH(3′)-IIIa in the absence (A) and presence (B) of CaATP. Other experimental conditions were as described in Figure 2. The raw data are shown in the upper panels, and plots of the heat of injection against the molar ratio of ligand to enzyme are shown in the lower panels with the best-fit lines to a one-site model. The steeper saturation curve in (B) yields more than a 6-fold higher association constant for the complex formation.

of backbone amide resonances were shifted with each aminoglycoside, suggesting that the conformation of the active site is altered to accommodate each aminoglycoside (Whittemore and Serpersu, unpublished data). Thus, the contribution of the enzyme to the determined ΔH_{int} may be different for each aminoglycoside.

Ternary Enzyme−CaATP−Aminoglycoside Complexes. An exothermic heat also accompanied titration of aminoglycosides into the enzyme−CaATP complex. However, the observed heat was significantly lower than the ΔH values observed in the binary titrations. As shown in Figure 3, the titration of ribostamycin into the solutions containing enzyme alone or the enzyme−CaATP complex exhibits different patterns. Comparison of aminoglycoside binding to APH(3′)-IIIa shows that binding is generally tighter or unchanged in the presence of CaATP (Tables 1 and 3). These results are in agreement with previous steady-state kinetics, viscosity, thio, and solvent isotope effect studies (*9*, *10*) suggesting a sequential substrate binding by a Theorell−Chance kinetic mechanism for APH(3′)-IIIa. It can also be suggested that the large exothermic heats observed in the formation of the binary enzyme−aminoglycoside complexes were mostly due to conformational changes in enzyme or ligand or both. Our earlier work showed that the enzyme-bound aminoglycosides, unlike their unbound forms, do not necessarily adopt the lowest energy conformation (*15*, *16*). Thus, binding to enzyme causes conformational changes in aminoglycosides. In addition, NMR spectra acquired with enzyme, enzyme−CaATP, enzyme−aminoglycoside, and enzyme−CaATP−aminoglycoside complexes, using uniformly ^{15}N-enriched APH(3′)-IIIa, showed that the binding of aminoglycosides to the APH(3′)-IIIa or APH(3′)-IIIa−CaATP caused a larger number of backbone resonances to shift when compared to the addition of CaATP to the enzyme or enzyme−aminoglycoside complex, suggesting that the binding of aminoglycoside causes significant conformational changes in the enzyme (Whittemore and Serpersu, unpublished data).

Table 3: Thermodynamic Parameters for Aminoglycoside Binding to APH(3′)-IIIa−CaATP (Ternary Complex) at pH 7.5[a]

	buffer	K_D (μM)	ΔH_{obs} (kcal/mol)	ΔH_{int}[b] (kcal/mol)	$-T\Delta S$ (kcal/mol)	ΔG (kcal/mol)	Δn[b]
kanamycin A	Tris	0.99	−9.4	−31.0	0.9	−8.5	1.85
	Bicine	1.3	−19.0		10.7	−8.3	
kanamycin B	Tris	0.22	−8.2	−29.1	−1.2	−9.4	1.79
	Bicine	0.39	−17.5		8.4	−9.1	
tobramycin	Tris	0.22	−9.1	−30.7	−0.3	−9.4	1.85
	Bicine	0.55	−18.7		9.8	−8.9	
amikacin	Tris	33.3	−4.8	−28.0	−1.5	−6.3	1.98
	Bicine	25.7	−15.1		8.6	−6.5	
ribostamycin	Tris	0.27	−11.6	−14.5	2.3	−9.3	0.25
	Bicine	0.53	−12.9		4.0	−8.9	
neomycin B	Tris	0.13	−12.2	−36.3	2.4	−9.8	2.06
	Bicine	0.30	−22.9		13.6	−9.3	
paromomycin I	Tris	0.16	−11.5	−27.9	1.8	−9.7	1.40
	Bicine	0.12	−18.8		9.0	−9.8	
lividomycin A	Tris	0.78	−10.5	−36.6	1.8	−8.7	2.23
	Bicine	0.55	−22.1		13.2	−8.9	

[a] Determined at 310 K. K_D values were calculated from ITC-derived K_A. Fitting errors: K_D, 2−12%; ΔH, 0.2−3%. The stoichiometry of complex formation was 1.0 ± 0.2 in all titrations. [b] Intrinsic enthalpy changes (ΔH_{int}) and net number of binding-coupled protons (Δn) were calculated using eqs 3a and 3b.

In the ternary complex formation, as was the case with the binary complexes, there were no trends separating the aminoglycosides with 4,5-disubstituted 2-DOS from those with 4,6-disubstituted 2-DOS with respect to the thermodynamic parameters. Overall, the entropic contribution was more favorable in the ternary complexes with all aminoglycosides when compared to the respective binary complexes. An explanation for this observation can be that the binding in the ternary complex is accompanied by expulsion of more water molecules from the binding interface when compared to the binary aminoglycoside−enzyme interaction. Thus, gain in entropy of the freed water molecules would provide a more favorable driving force for the formation of the ternary complex. Alternatively, more favorable entropic contribution

may come from the increased hydrophobic interactions between the enzyme and the ligands. It is already shown in the crystal structure of the enzyme with substrates (*7*) that the adenine moiety of MgADP is involved in a stacking interaction with the aromatic ring of the Tyr 42. This interaction is absent in the binary enzyme−aminoglycoside complex.

The spread between the lowest and highest affinity toward the enzyme was somewhat narrower in ternary complexes. Overall, ΔG value for each antibiotic was only slightly more negative in the ternary complexes when compared to the respective binary complexes. In the ternary complexes, more uniform Δn values were obtained, and the values of ΔH_{int} varied between −14.5 and −36.6 kcal/mol. The analysis of these values, however, is even more complicated than those of the binary complexes due to contributions that may result from the interactions of ATP with protein and ligand coordination to the metal ion. On the other hand, comparison of the dissociation constants of various enzyme−aminoglycoside complexes (a thermodynamic property which is not directly correlated to the heat of reaction) with several aminoglycosides that have a structural difference of either a single functional group or a complete sugar ring between two aminoglycosides afforded some clues about the roles of these groups in enzyme−aminoglycoside interactions. Several specific comparisons are presented in the following paragraphs.

2′-Amino vs Hydroxyl. Kanamycin A and kanamycin B differ only by the presence of an amino group at the 2′-position of kanamycin B instead of the hydroxyl in kanamycin A (Figure 1). ΔH_{int} is 3.6 kcal/mol less negative with kanamycin B when compared to kanamycin A in the binary enzyme−aminoglycoside complex (Table 1), while the affinity of kanamycin B to the enzyme is ∼15-fold higher than that of kanamycin A. These differences between the kanamycins are significantly reduced in the ternary complexes (Table 3). If one assumes the ability of the protonated (or unprotonated) amino group to engage in one or more hydrogen bonds than the hydroxyl group, then the expected ΔH should have been more negative with kanamycin B. On the other hand, formation of additional hydrogen bonds mediated by the 2′-amino group may weaken the strength of other favorable interactions, i.e., altered cooperativity among hydrogen bonds, causing a less enthalphically driven complex formation for kanamycin B. Alternatively, the more negative ΔH with kanamycin A may be the result of larger conformational changes in enzyme or antibiotic or both. If the protonated amino group is involved in ionic interactions with the protein side chains, then this would provide more positive entropic contribution to the binding through desolvation. The second alternative appears to account for the relatively more favorable entropic terms in the binary and ternary complexes of kanamycin B with respect to kanamycin A.

A crystal structure for the binary kanamycin−APH(3′)-IIIa complex is not available; however, the crystal structure of the ternary APH(3′)-IIIa−MgADP−kanamycin A complex is available (*7*). Examination of the crystal structure reveals that the closest enzyme atom to the 2′-hydroxyl oxygen is the side chain carboxyl oxygen of Asp 190 at a distance of 4.2 Å in the ternary complex (Figure 4), and therefore the 2′-position was not considered among the

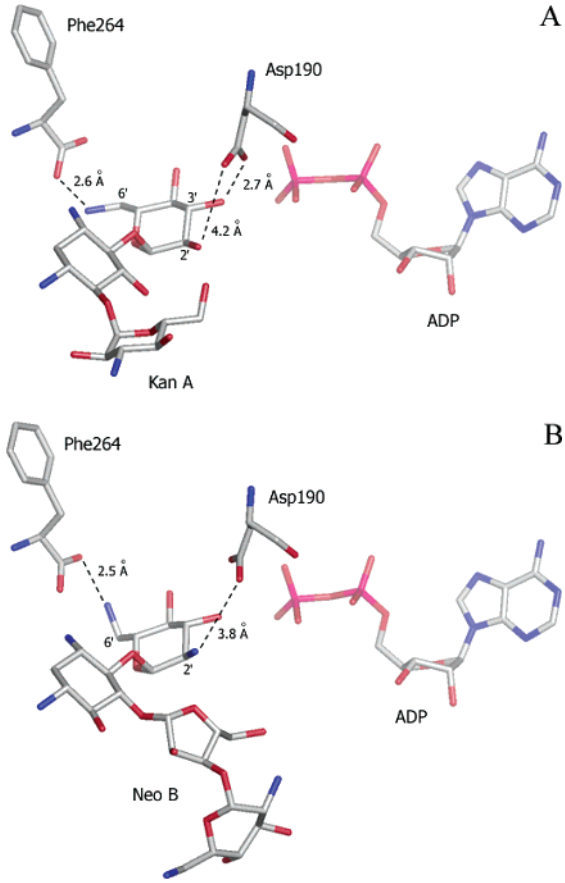

FIGURE 4: Crystal structures of (A) kanamycin A and (B) neomycin B complexed with ADP and APH(3′)-IIIa (*7*). Images were produced by Deep View (*35*) and Pymol (*36*). The relevant distances between ligand functional groups and enzyme residues are indicated with dotted lines.

enzyme contacts in previous structural analyses (*7*). Our results suggest that the 2′-amino group of kanamycin B is involved in enzyme−ligand interactions and makes more favorable contacts possibly with Asp 190 either through hydrogen bonding or electrostatic interactions or both to yield more negative ΔG values for the binary and ternary complexes of kanamycin B when compared to the respective complexes of kanamycin A. The pK_a of the 2′-amino group is ∼8.6 (*33*), which is the highest of all amine groups on kanamycin B. At pH 7.5 only the 2′-amino group would be ∼90% protonated while all others would be ∼50% or less protonated. Experiments performed with the ternary complexes at pH 8.5 (Figure 5) showed that ΔH_{int} for kanamycin A was only slighty changed, while it became significantly more negative for kanamycin B. The entropic contributions were reversed in both cases and became more disfavored with kanamycin B (Table 4). At this pH only the 2′-amino group of unbound kanamycin B would be ∼50% protonated while the others are only ∼10% protonated. Since kanamycin A lacks the 2′-amino group, at pH 8.5, all of its amino groups would be only about 10% protonated. This suggests that charged amino groups of aminoglycosides provide favorable binding interactions in enzyme−aminoglycoside complexes. These observations are also consistent with the involvement of the charged 2′-amino group in enzyme−kanamycin B interactions. The determined $\Delta\Delta n$ value between the kanamycins is 0.8 at pH 8.5. This value, again, exceeds the total protonation capacity of the 2′-amino group and suggests that

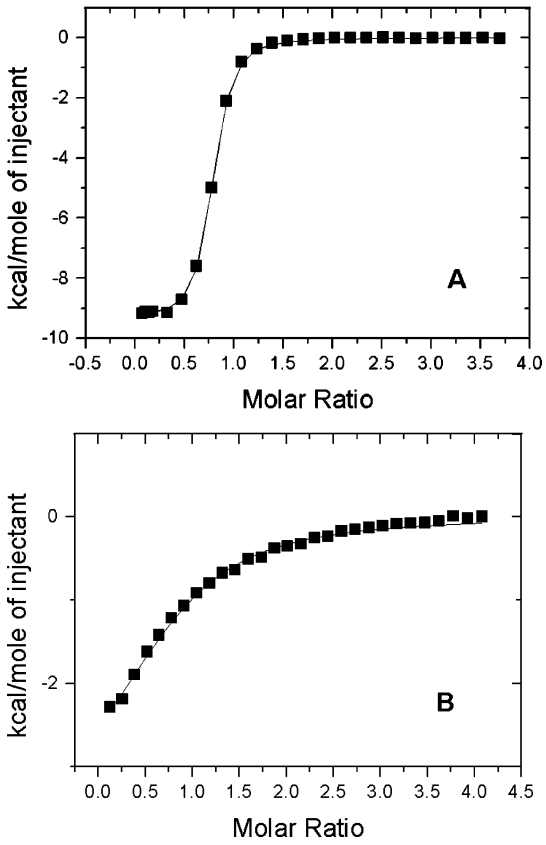

FIGURE 5: Heat of injection observed in the titration of kanamycin A to 80 μM APH(3′)-IIIa in the presence of CaATP at 7.5 (A) and 8.5 (B). Other experimental conditions were as described in Figure 2. The solid line represents the best fit to the data using a one-site binding model.

Table 4: Thermodynamic Parameters for Aminoglycoside Binding to APH(3′)-IIIa−CaATP (Ternary Complex) at pH 8.5[a]

	buffer	K_D (μM)	ΔH_{obs} (kcal/mol)	ΔH_{int}[b] (kcal/mol)	$-T\Delta S$ (kcal/mol)	ΔG (kcal/mol)	Δn[b]
kanamycin A	Tris	28.3	−3.7	−34.1	−2.8	−6.5	2.60
	Bicine	24.2	−17.2		10.7	−6.5	
kanamycin B	Tris	9.4	−8.5	−48.3	1.3	−7.1	3.40
	Bicine	4.4	−26.2		18.6	−7.6	
tobramycin	Tris	12.6	−7.0	−48.4	0.09	−7.0	3.54
	Bicine	5.6	−25.4		18.0	−7.4	
neomycin B	Tris	0.40	−11.1	−55.7	2.2	−8.9	3.81
	Bicine	0.17	−30.9		21.3	−9.6	
paromomycin I	Tris	3.7	−10.9	−48.9	3.1	−7.8	3.25
	Bicine	1.88	−27.8		19.7	−8.1	

[a] Determined at 310 K. K_D values were calculated from ITC-derived K_A. Fitting errors: K_D, 2−10%; ΔH, 0.5−6%. The stoichiometry of complex formation was 1.0 ± 0.2 in all titrations. [b] Intrinsic enthalpy changes (ΔH_{int}) and net number of binding-coupled protons (Δn) were calculated using eqs 3a and 3b.

other groups must be involved. These results also suggest that even very small structural differences between ligands may alter other enzyme−ligand interactions involving the similar structural parts of ligands (i.e., increased or decreased cooperativity among the hydrogen bonds). Thus observed changes in the thermodynamic parameters may not easily be reconciled in a quantitative manner.

6′-Amino vs Hydroxyl. The presence of an amino or hydroxyl group at the 6′-position is the only difference between neomycin B (amine) and paromomycin I (hydroxyl) (Figure 1). Binary complexes of both aminoglycosides with the enzyme exhibit similar K_D values, but their intrinsic binding enthalpies differ by 13.4 kcal/mol (Table 1). However, when the ternary titrations were performed at pH 8.5, at which only the 6′-amino group would be ∼50% protonated while the others are in a ∼10% protonated state, significant differences were observed between the binding pattern of two antibiotics. The dissociation constant of paromomycin I from the ternary APH(3′)-IIIa−CaATP−paromomycin I complex was increased by ∼20-fold, while the same effect was only 1.3-fold for neomycin B. This observation suggests that the remaining charge on the 6′-amino group of neomycin B is responsible for the ∼10-fold tighter binding of this antibiotic to the enzyme when compared to paromomycin I at pH 8.5. Thus, the 6′-amino group must be involved in enzyme−aminoglycoside interactions, and it contributes 1.3 kcal/mol favorably to ΔG when it is in the ∼50% protonated state. Although the determined $\Delta\Delta n$ value of 0.56 can be attributed to the protonation of the 6′-amino group alone, as indicated above, this may be coincidental, and contributions due to protonation/deprotonation of other groups cannot be ruled out.

The crystal structure of the ternary APH(3′)-IIIa−MgADP−neomycin B complex shows that the 6′-amino group is 2.6 Å away from one of the carboxyl oxygens of the C-terminal residue Phe 264 (Figure 4). Entropic contributions are similar in the ternary complexes of neomycin B and paramomycin I at pH 8.5. Thus, the observed difference in ΔG is solely due to the difference in ΔH, and it may reflect the ability of the amino group to form more hydrogen bonds than the hydroxyl group with Phe 264.

The importance of the 2′- and the 6′-amino groups is also supported by the chemical modification studies in which particular amino groups were one-by-one deaminated to study their role in enzyme catalysis (*34*). Elimination of the 2′- and the 6′-amino groups was shown to increase K_m and bring about 10- and 30-fold losses of catalytic efficiency of APH(3′)-IIIa, respectively. In this work, we showed that even replacement of these amino groups by hydroxyl groups still shows significant effects on the thermodynamic properties of the binary and ternary enzyme−aminoglycoside complexes.

3′-Deoxy vs Hydroxyl. Tobramycin, a competitive inhibitor of APH(3′)-IIIa, lacks the 3′-hydroxyl group of kanamycin B and therefore cannot be modified by the enzyme. Comparison of K_D for tobramycin and kanamycin B shows that the presence or absence of a hydroxyl group at the 3′-position does not have an effect on the affinity of aminoglycoside to the enzyme−metal-ATP complex. As was the case with kanamycin A vs kanamycin B, there were differences between the thermodynamic parameters of the binary complexes of kanamycin B and tobramycin with APH(3′)-IIIa (Table 1). Kanamycin B exhibited lower ΔH and $T\Delta S$ values in the binary complex. These differences disappeared almost completely in the ternary complexes, yielding not only identical ΔG and K_D values but also similar ΔH and $T\Delta S$ values (Table 3). These observations suggest that once the nucleotide-binding site is occupied, the 3′-hydroxyl group has no significant contribution to the thermodynamic parameters. This is somewhat surprising since the 3′-OH is the point of modification by APH(3′)-IIIa, and it is located near the catalytically required residue Asp 190 (Figure 4). Thus,

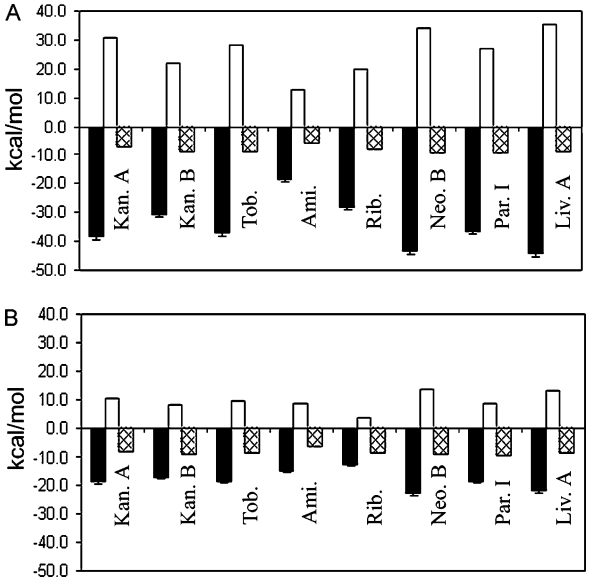

FIGURE 6: Thermodynamic parameters of aminoglycoside binding to (A) APH(3′)-IIIa and (B) the APH(3′)-IIIa−CaATP complex at 310 K in Bicine buffer. Bars represent ΔH (black), $-T\Delta S$ (white), and ΔG (crossed). Abbreviations: Kan. A, kanamycin A; Kan. B, kanamycin B; Tob., tobramycin; Ami., amikacin; Rib., ribostamycin; Neo. B, neomycin B; Par. I, paromomycin I; Liv. A, lividomycin A.

one would expect this group to be positioned precisely for a nucleophilic attack on the γ-phosphoryl group of ATP via interaction(s) with Asp 190. A plausible explanation may be that the removal of the hydroxyl group leads to stronger interactions via other existing hydrogen bonds between the aminoglycoside and the enzyme and/or alters the organization of water in the active site, which compensates for the loss of a hydrogen bond through the 3′-hydroxyl. These results, again, clearly suggest that interpretation of thermodynamic data, even for very similar compounds, may not be straightforward, and detailed structural information on the complexes of each compound is necessary for a more quantitative interpretation.

Size of Substrates. Comparison of thermodynamic parameters of the binary and ternary complexes of ribostamycin (three rings), neomycinB/paramomycin I (four rings), and lividomycin A (five rings) shows that the determined ΔH_{int} is significantly different for ribostamycin. Since ribostamycin is the smallest of them, these observations suggest that the fourth rings of the longer aminoglycosides contribute to binding. Examination of the data also yields that the fifth ring of lividomycin A does not contribute to binding. The crystal structure of the APH(3′)-IIIa−MgADP−neomycin B complex (*7*) shows that the side chain nitrogens and oxygens of Asn 134, Asp 193, Ser 194, and Glu 230 are within 4 Å distance of the fourth ring of neomycin B. Thus one or more of these side chains may interact with this ring.

Enthalpy−Entropy Compensation. The determined ΔH_{obs} and $T\Delta S$ values were plotted for the binary and the ternary complexes to investigate the enthalpy−entropy compensation of the aminoglycoside binding to APH(3′)-IIIa. Enthalpy−entropy compensation for the formation of the binary and ternary complexes of each aminoglycoside are shown in Figures 6 and 7. Plots of enthalpy−entropy compensation with a slope of unity indicate that changes in binding enthalpies ($\Delta\Delta H$) are equally compensated by changes in

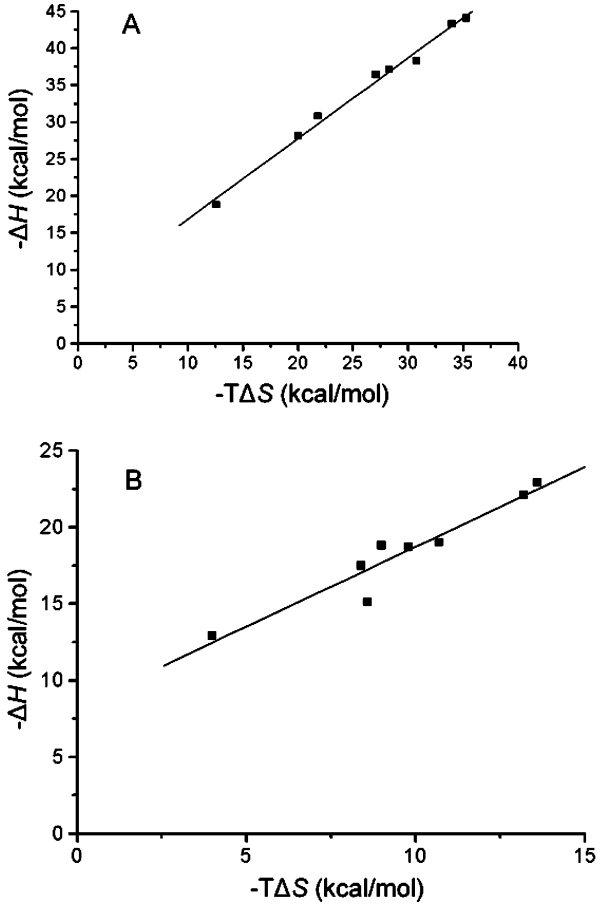

FIGURE 7: Enthalpy−entropy compensation plots constructed by linear regression analysis of binding data from Tables 1 and 3. (A) Binary enzyme−aminoglycoside complexes (slope = 1.09, R = 0.99) and (B) ternary enzyme−CaATP−aminoglycoside complexes (slope = 1.04, R = 0.96).

binding entropies ($\Delta\Delta S$) between the different ligands of an enzyme. If $\Delta\Delta H$ is greater than $\Delta\Delta S$, a slope greater than unity is obtained. In the case where $\Delta\Delta H$ is smaller than the $\Delta\Delta S$, the slope is smaller than unity. Such plots for binary and ternary complexes of APH(3′)-IIIa with substrates yielded slopes of 1.09 and 1.04, respectively (Figure 7), indicating that, in both cases, changes in binding enthalpies of different aminoglycosides are equally compensated by the changes in their entropic terms.

CONCLUSIONS

With the exception of amikacin, the free energies of formation for the binary enzyme−aminoglycoside and the ternary enzyme−CaATP−aminoglycoside complexes were similar to each other regardless of the structure of the aminoglycosides involved. The heat of formation and the entropic contribution to complex formation, however, showed significant variation among the aminoglycosides. The formation of all binary complexes exhibits large negative ΔH values with strongly disfavored entropic contribution. This is significantly different from the aminoglycoside−RNA interactions that show favorable entropic contribution to the complex formation (*28*). The formation of ternary complexes, on the other hand, was entropically more favored when compared to the binary complexes. Overall, there were no strong correlations between the thermodynamic parameters and the size of the aminoglycosides, or the kinetic param-

eters, or the substitution pattern of the 2-DOS ring (4,5 vs 4,6). Also, comparisons between structurally very similar aminoglycosides showed that the presence of an amino or hydroxyl group at the 2′- and the 6′-positions affected the thermodynamic properties of various enzyme−aminoglycoside complexes significantly, while the lack of a hydroxyl group at the 3′-position had no detectable effect. Similarly, additional sugar rings of larger aminoglycosides beyond the fourth ring appear to have no significant effect on the thermodynamic properties of enzyme−aminoglycoside complexes.

REFERENCES

1. Davies, J. E. (1991) in *Antibiotics in Laboratory Medicine* (Lorian, V., Ed.) pp 691−713, Williams and Wilkins, Baltimore, MD.
2. Mingeot-Leclercq, M. P., Glupczynski, Y., and Tulkens, P. M. (1999) Aminoglycosides: activity and resistance, *Antimicrob. Agents Chemother. 43*, 727−737.
3. Umezawa, H. (1974) in *Advances in Carbohydrate Chemistry and Biochemistry* (Tipson, R. S., and Horton, D., Eds.) pp 183−225, Academic Press, New York, San Francisco, and London.
4. Moazed, D., and Noller, H. F. (1987) Interaction of antibiotics with functional sites in 16S ribosomal RNA, *Nature 327*, 389−394.
5. Davies, J. (1994) Inactivation of antibiotics and the dissemination of resistance genes, *Science 264*, 375−382.
6. Shaw, K. J., Rather, P. N., Hare, R. S., and Miller, G. H. (1993) Molecular genetics of aminoglycoside resistance genes and familial relationships of the aminoglycoside-modifying enzymes, *Microbiol. Rev. 57*, 138−163.
7. Fong, D. H., and Berghuis, A. M. (2002) Substrate promiscuity of an aminoglycoside antibiotic resistance enzyme via target mimicry, *EMBO J. 21*, 2323−2331.
8. McKay, G. A., Thompson, P. R., and Wright, G. D. (1994) Broad spectrum aminoglycoside phosphotransferase type III from *Enterococcus*: overexpression, purification, and substrate specificity, *Biochemistry 33*, 6936−6944.
9. McKay, G. A., and Wright, G. D. (1995) Kinetic mechanism of aminoglycoside phosphotransferase type IIIa. Evidence for a Theorell-Chance mechanism, *J. Biol. Chem. 270*, 24686−24692.
10. McKay, G. A., and Wright, G. D. (1996) Catalytic mechanism of enterococcal kanamycin kinase (APH(3′)-IIIa): viscosity, thio, and solvent isotope effects support a Theorell-Chance mechanism, *Biochemistry 35*, 8680−8685.
11. Boehr, D. D., Thompson, P. R., and Wright, G. D. (2001) Molecular mechanism of aminoglycoside antibiotic kinase APH(3′)-IIIa: roles of conserved active site residues, *J. Biol. Chem. 276*, 23929−23936.
12. Burk, D. L., Hon, W. C., Leung, A. K., and Berghuis, A. M. (2001) Structural analyses of nucleotide binding to an aminoglycoside phosphotransferase, *Biochemistry 40*, 8756−8764.
13. Cox, J. R., McKay, G. A., Wright, G. D., and Serpersu, E. H. (1996) Arrangement of substrates at the active site of an aminoglycoside antibiotic 3′-phosphotransferase as determined by NMR, *J. Am. Chem. Soc. 118*, 1295−1301.
14. Cox, J. R., and Serpersu, E. H. (1997) Biologically important conformations of aminoglycoside antibiotics bound to an aminoglycoside 3′-phosphotransferase as determined by transferred nuclear Overhauser effect spectroscopy, *Biochemistry 36*, 2353−2359.
15. DiGiammarino, E. L., Draker, K. A., Wright, G. D., and Serpersu, E. H. (1998) Solution studies of isepamicin and conformational comparisons between isepamicin and butirosin A when bound to an aminoglycoside 6′-*N*-acetyltransferase determined by NMR spectroscopy, *Biochemistry 37*, 3638−3644.
16. Mohler, M. L., Cox, J. R., and Serpersu, E. H. (1998) Aminoglycoside phosphotransferase(3′)-IIIa (APH(3′)-IIIa)-bound conformation of the aminoglycoside lividomycin A characterized by NMR, *Carbohydr. Lett. 3*, 17−24.
17. Cox, J. R., Ekman, D. R., DiGiammarino, E. L., Akal-Strader, A., and Serpersu, E. H. (2000) Aminoglycoside antibiotics bound to aminoglycoside-detoxifying enzymes and RNA adopt similar conformations, *Cell Biochem. Biophys. 33*, 297−308.
18. Boehr, D. D., Farley, A. R., Wright, G. D., and Cox, J. R. (2002) Analysis of the pi-pi stacking interactions between the aminoglycoside antibiotic kinase APH(3′)-IIIa and its nucleotide ligands, *Chem. Biol. 9*, 1209−1217.
19. Ozen, C., and Serpersu, E. H. (2004) *Annual Meeting Abstracts Issue*, p 495-Pos, Biophysical Society, Bethesda, MD.
20. Wiseman, T., Williston, S., Brandts, J. F., and Lin, L. N. (1989) Rapid measurement of binding constants and heats of binding using a new titration calorimeter, *Anal. Biochem. 179*, 131−137.
21. Ladbury, J. E., and Chowdhry, B. Z. (1996) Sensing the heat: the application of isothermal titration calorimetry to thermodynamic studies of biomolecular interactions, *Chem. Biol. 3*, 791−801.
22. Jelesarov, I., and Bosshard, H. R. (1999) Isothermal titration calorimetry and differential scanning calorimetry as complementary tools to investigate the energetics of biomolecular recognition, *J. Mol. Recognit. 12*, 3−18.
23. Leavitt, S., and Freire, E. (2001) Direct measurement of protein binding energetics by isothermal titration calorimetry, *Curr. Opin. Struct. Biol. 11*, 560−566.
24. Surolia, A., Sharon, N., and Schwarz, F. P. (1996) Thermodynamics of monosaccharide and disaccharide binding to *Erythrina corallodendron* lectin, *J. Biol. Chem. 271*, 17697−17703.
25. Dam, T. K., and Brewer, C. F. (2002) Thermodynamic studies of lectin-carbohydrate interactions by isothermal titration calorimetry, *Chem. Rev. 102*, 387−429.
26. Chervenak, M. C., and Toone, E. J. (1995) Calorimetric analysis of the binding of lectins with overlapping carbohydrate-binding ligand specificities, *Biochemistry 34*, 5685−5695.
27. Xie, H., Bolam, D. N., Nagy, T., Szabo, L., Cooper, A., Simpson, P. J., Lakey, J. H., Williamson, M. P., and Gilbert, H. J. (2001) Role of hydrogen bonding in the interaction between a xylan binding module and xylan, *Biochemistry 40*, 5700−5707.
28. Kaul, M., Barbieri, C. M., Kerrigan, J. E., and Pilch, D. S. (2003) Coupling of drug protonation to the specific binding of aminoglycosides to the A site of 16 S rRNA: elucidation of the number of drug amino groups involved and their identities, *J. Mol. Biol. 326*, 1373−1387.
29. Hegde, S. S., Dam, T. K., Brewer, C. F., and Blanchard, J. S. (2002) Thermodynamics of aminoglycoside and acyl-coenzyme A binding to the *Salmonella enterica* AAC(6′)-Iy aminoglycoside *N*-acetyltransferase, *Biochemistry 41*, 7519−7527.
30. Bernhard, S. A. (1956) Ionization constants and heats of tris-(hydroxymethyl)aminomethane and phosphate buffers, *J. Biol. Chem. 218*, 961−969.
31. Fukada, H., and Takahashi, K. (1998) Enthalpy and heat capacity changes for the proton dissociation of various buffer components in 0.1 M potassium chloride, *Proteins 33*, 159−166.
32. Doyle, M. L., Louie, G., Dal Monte, P. R., and Sokoloski, T. D. (1995) Tight binding affinities determined from thermodynamic linkage to protons by titration calorimetry, *Methods Enzymol. 259*, 183−194.
33. Walter, F., Vicens, Q., and Westhof, E. (1999) Aminoglycoside-RNA interactions, *Curr. Opin. Chem. Biol. 3*, 694−704.
34. McKay, G. A., Roestamadji, J., Mobashery, S., and Wright, G. D. (1996) Recognition of aminoglycoside antibiotics by enterococcal-staphylococcal aminoglycoside 3′-phosphotransferase type IIIa: role of substrate amino groups, *Antimicrob. Agents Chemother. 40*, 2648−2650.
35. Guex, N., and Peitsch, M. C. (1997) SWISS-MODEL and the Swiss-PdbViewer: an environment for comparative protein modeling, *Electrophoresis 18*, 2714−2723.
36. Delano, W. L. (2002) *The PyMol Molecular Graphics System*, DeLano Scientific, San Carlos, CA.

BI0487286